

## **Generation of Isotropic and Anisotropic Scattering Cross Sections for Boltzmann-Fokker-Planck Equation via Decomposition and Minimized RMS Errors**

**Jong Woon Kim and Nam Zin Cho**

Korea Advanced Institute of Science and Technology  
Department of Nuclear Engineering  
373-1 Kusong-dong, Yusong-gu  
Taejeon, Korea 305-701  
Email : nzcho@mail.kaist.ac.kr

### **Abstract**

Handling the highly anisotropic scattering of fast neutrons with conventional methods usually means that high-order Legendre expansions are necessary to obtain correct angular fluxes. This drawback in standard transport calculations is avoided by applying the Boltzmann-Fokker-Planck (BFP) equation approach which has been used in both neutral and charged-particle transport problems.

Previously, Caro and Ligou, and Morel have introduced Fokker-Planck decomposition methods, which decompose elastic scattering cross section into forward-peaked and smooth components.

A new method for decomposing scattering cross sections for Boltzmann-Fokker-Planck equation is presented. We start from the basic data  $\sigma_s(\mu)$  (given by ENDF/B-VI) to get more correctly determined BFP data. In this method, we use Legendre expansion for smooth component and exponential function, which Caro and Ligou used in their paper, for forward-peaked component. In addition, by using RMS errors and an extra degree of freedom ( $Y$ ), we conserve both moment and scattering cross section.

### **1. Introduction**

When we use the Boltzmann transport equation to treat neutral and charged-particle transport problems, a Legendre expansion is used to represent scattering cross section with the assumption that scattering is almost isotropic. However, when we deal with high energy particle (above  $\sim 5\text{MeV}$ ), it is hard to get accurate solutions with this assumption since differential scattering cross sections are very anisotropic.

The basic idea of the BFP (Boltzmann-Fokker-Planck) equation approach is to decompose a highly forward-peaked differential scattering cross section into the sum of a forward-peaked cross section and a smooth or nonpeaked cross section. This approach often gives accurate solutions at a reasonable computational cost. In principle, this approach is superior to the pure Boltzmann approach. The smooth cross section should be well represented with a

Legendre expansion of reasonably low order, and the Fokker-Planck approximation should be accurate for the forward-peaked cross section, whereas a Legendre expansion of reasonable order is usually inadequate to represent the complete scattering cross section.

For the BFP equation, it is necessary to decompose a highly forward-peaked differential scattering into a forward-peaked cross section and a smooth or nonpeaked cross section. Over the last several years, Caro and Ligou, and Morel have introduced Fokker-Planck decomposition methods.

A new approach in this paper is based on the basic data  $\sigma_s(\mu)$  (given by ENDF/B-VI) [3][4] to accurately determine BFP data. In order to obtain an accurate representation of scattering cross section over the full interval  $[-1, +1]$ , we make the most of characteristics of exponential function and Legendre expansion. The exponential function is used for representing forward-peaked scattering cross section, and the Legendre expansion is used for representing smooth scattering cross section in that smooth scattering cross section consists of several hills and valleys. In addition to that, by using RMS errors and an extra degree of freedom ( $Y$ ), we try to conserve both moment and scattering cross section.

Brief descriptions of previous methods, which are C-L method, the moment-based (MB) method, and the partial-range fitting (PRF) method, are given in Section 2. The details of the new decomposition method are described in Section 3. Computational results are given in Section 4, and conclusions are given in Section 5.

## 2. Brief descriptions of previous methods

### 2.1 Caro and Ligou's method (C-L method)

Caro and Ligou presented a Fokker-Planck decomposition technique that is completely defined in terms of the Legendre moments available in standard cross-section libraries[1]. In their method, they use exponential function to represent both forward-peaked cross section and smooth or nonpeaked cross section.

The basic function is

$$h(\mu, \tau) = \tau \exp[-\tau(1 - \mu)]. \quad (1)$$

With Eq.(1), forward-peaked cross section is represented as

$$\sigma_s^{II}(\mu) = K'' h(\mu, \tau''), \quad (2)$$

and smooth cross section as

$$\sigma_s^I(\mu) = K' h(\mu, \tau'), \quad (3)$$

where  $K''$ ,  $\tau''$  and  $K'$ ,  $\tau'$  refer, respectively, to the singular and smooth part parameters and  $\mu$  is angular cosine in center of mass system.

The corresponding Legendre moments:

$$\sigma_{s,l} = \underbrace{2\pi K'' h_l(\tau'')}_{singular} + \underbrace{2\pi K' h_l(\tau')}_{smooth}. \quad (4)$$

The first and second term of Eq.(4) are singular and smooth moment, respectively.

An exponential function is suitable for fitting forward-peaked cross section. However, it is inadequate for an accurate representation of smooth or nonpeaked cross section.

## 2.2 Morel's moment-based method (MB method)

This method is quite similar to the C-L method in that the last two moments of the complete cross-section expansion are used to define the singular component. The fundamental difference between MB method[2] and C-L method is that the moments of the singular component are given by the Fokker-Planck moments rather than by an exponential function:

$$\sigma_l^{II} = \sigma_0^{II} - \frac{\alpha}{2}[l(l+1)]. \quad (5)$$

There are two parameters in Eq.(5); the zeroth moment of the singular component:  $\sigma_0^{II}$  and the restricted momentum transfer:  $\alpha$ . Linear equations for these parameters are obtained by equating  $\sigma_L$  and  $\sigma_{L-1}$  with  $\sigma_L^{II}$  and  $\sigma_{L-1}^{II}$ , respectively.

Because this decomposition technique is entirely defined in terms of the Legendre moments of the complete cross section, we refer to it as the moment-based (MB) method.

## 2.3 Morel's partial-range fitting (PRF) method

This cross-section decomposition method[2] is quite different from the previously discussed methods. This method does not generate the moments of the smooth component from the moments of the complete cross section, but rather generates them directly from the complete cross section itself. Morel determines the Legendre moments of the smooth component on the interval  $[-1, +1]$  by doing a least-squares fit on a subinterval  $[-1, \mu_b]$ , where the parameter  $\mu_b$  is less than unity. The parameter  $\mu_b$  is chosen to obtain accurate polynomial fit over the subinterval and to ensure that  $\mu_b$  corresponds to a "small" scattering angle.

To get partial-range smooth coefficients, the error in the fit is

$$Error = \int_{-1}^{\mu_b} \left[ \sigma_s(\mu_0) - \sum_{l=0}^L \frac{2l+1}{2} \sigma_l P_l(\mu_0) \right]^2 d\mu_0, \quad (6)$$

where  $\sigma_s(\mu_0)$  is given data.

This method is superior to the previous methods in terms of accuracy in charged-particle case. However, if the cross section behaves irregularly, that is in neutron scattering case, PRF method cannot give the same superior results as charged-particle case. In other words, it is hard to predict the behavior of the outside of the interval  $[-1, \mu_b]$  with PRF method since the smooth scattering cross section of full-range expansion is very sensitive to the value of parameter  $\mu_b$  in neutron scattering case.

## 3. New decomposition method

We now introduce a new method for performing cross-section decompositions. This method requires cross-section data that may be much less accessible than that available in standard moment libraries. That is to say, the basic data  $\sigma_s(\mu)$  is given by ENDF/B-VI. An exponential fitting is used for forward-peak scattering cross section, and a Legendre expansion is used for smooth component. Smooth moment  $\sigma_l^I$  and singular moment  $\sigma_l^{II}$  are obtained independently rather than by subtraction. We also try to conserve both moment and scattering cross section by minimizing RMS errors of moment and scattering cross section.

We want to minimize RMS errors of moment and scattering cross section as follows:  
RMS for moment:

$$Min \sqrt{\frac{1}{L+1} \sum_{l=0}^L [\sigma_l - (\sigma_l^I + \sigma_l^{II})]^2}. \quad (7)$$

RMS for scattering cross section:

$$Min \sqrt{\frac{1}{N+1} \sum_{i=0}^N [\sigma(\mu_i) - (\sigma^I(\mu_i) + \sigma^{II}(\mu_i))]^2}. \quad (8)$$

Smooth component will be discussed first, and singular component will be followed.

### 3.1 Smooth component

In this new method, Legendre expansion is used to deal with smooth component. Smooth scattering cross section  $\sigma^I(\mu)$  and smooth moment  $\sigma_l^I$  are defined as follows:

Smooth scattering cross section:

$$\sigma^I(\mu) = \sum_{l=0}^L \frac{2l+1}{2} \sigma_{s,l} P_l(\mu). \quad (9)$$

Smooth moment:

$$\sigma_l^I = 2\pi \sigma_{s,l}. \quad (10)$$

We fit both elastic scattering cross section that is based on ENDF/B-VI on the interval  $[-1, \mu_b]$  and extrapolation exponential function that is optimized by RMS errors on the interval  $[\mu_b, +1]$  with Eq.(9).

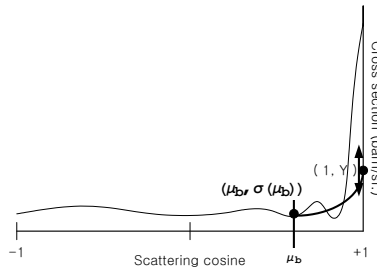


Figure 1: A degree of freedom,  $Y$ .

Parameter  $\mu_b$  is obtained by differentiating elastic scattering cross section that is based on ENDF/B-VI.

$$\frac{d}{d\mu} \left[ \frac{\sigma_s(E)}{2\pi} \sum_{l=0}^{NL} \frac{2l+1}{2} a_l(E) P_l(\mu) \right] = 0. \quad (11)$$

Among  $\mu$ 's that satisfy Eq.(11), the third value (the second valley from  $\mu = 1.0$ ) is defined as  $\mu_b$  in this method.

The elastic scattering cross section to fit on the interval  $[-1, \mu_b]$  with Eq.(9) is

$$\sigma(\mu) = \frac{\sigma_s(E)}{2\pi} \sum_{l=0}^{NL} \frac{2l+1}{2} a_l(E) P_l(\mu), \quad (12)$$

where  $\sigma_s(E)$ ,  $NL$ , and  $a_l(E)$  are given in ENDF/B-VI.

The extrapolation exponential function to fit on the interval  $[\mu_b, +1]$  with Eq.(9) is

$$\sigma(\mu) = K^I \tau^I \exp\{-\tau^I(1 - \mu)\}, \quad (13)$$

where  $K^I$  and  $\tau^I$  are determined as follows. If we use  $(1, Y)$  and  $(\mu_b, \sigma(\mu_b))$  in Fig. 1 with Eq.(13), then

$$Y = K^I \tau^I \exp\{-\tau^I(1 - 1)\}, \quad (14)$$

where  $Y$  is varying from 0 to 2.0 to minimize RMS errors, and

$$\sigma(\mu_b) = K^I \tau^I \exp\{-\tau^I(1 - \mu_b)\}. \quad (15)$$

Dividing Eq.(15) by Eq.(14),

$$\frac{\sigma(\mu_b)}{Y} = \frac{K^I \tau^I \exp\{-\tau^I(1 - \mu_b)\}}{K^I \tau^I}. \quad (16)$$

From Eqs.(14) and (16), we can determine  $\tau^I$  and  $K^I$  for extrapolation exponential function:

$$\tau^I = \frac{1}{\mu_b - 1} \ln \left( \frac{\sigma(\mu_b)}{Y} \right), \quad (17)$$

and

$$K^I = \frac{Y}{\tau^I}. \quad (18)$$

Let Eq.(9) be equal to Eq.(12) and Eq.(13) for each interval, respectively,

$$F(\mu) = \sum_{l=0}^L \frac{2l+1}{2} \sigma_{s,l} P_l(\mu), \quad (19)$$

where

$$F(\mu) = \begin{cases} \frac{\sigma_s(E)}{2\pi} \sum_{l=0}^{NL} \frac{2l+1}{2} a_l(E) P_l(\mu), & -1 \leq \mu \leq \mu_b, \\ K^I \tau^I \exp\{-\tau^I(1 - \mu)\}, & \mu_b \leq \mu \leq 1. \end{cases} \quad (20)$$

Multiplying Eq.(19) by  $P_k(\mu)$  and integrating over  $-1$  to  $+1$ , we obtain

$$\begin{aligned}\int_{-1}^{+1} F(\mu)P_k(\mu)d\mu &= \int_{-1}^{+1} \sum_{l=0}^L \frac{2l+1}{2} \sigma_{s,l} P_l(\mu)P_k(\mu)d\mu \\ &= \frac{2k+1}{2} \sigma_{s,k} \int_{-1}^{+1} P_k(\mu)P_k(\mu)d\mu \\ &= \sigma_{s,k}\end{aligned}\tag{21}$$

Changing index  $k$  to  $l$ , we obtain

$$\sigma_{s,l} = \int_{-1}^{+1} F(\mu)P_l(\mu)d\mu.\tag{22}$$

With  $\sigma_{s,l}$ , we can determine smooth scattering cross section by Eq.(9) and smooth moment by Eq.(10).

### 3.2 Singular component

We use an exponential function to fit forward-peaked scattering cross section in this method since exponential function is suitable for fitting a highly forward peak. We subtract smooth scattering cross section from ENDF scattering cross section to fit the remainders. Singular scattering cross section  $\sigma^{II}(\mu)$  and singular moment  $\sigma_l^{II}$  are defined as follows:

Singular scattering cross section:

$$\sigma^{II}(\mu) = K^{II} \tau^{II} \exp\{-\tau^{II}(1-\mu)\}.\tag{23}$$

Singular moment:

$$\sigma_l^{II} = 2\pi K^{II} h_l(\tau^{II}).\tag{24}$$

where  $K^{II}$  and  $\tau^{II}$  are singular parameters.

To determine  $K^{II}$  and  $\tau^{II}$ , we need two conditions.

- Condition 1:

By subtracting smooth scattering cross section from ENDF scattering cross section, we obtain singular scattering cross section at  $\mu = 1.0$ :

$$\sigma^{II}(1.0) = \sigma(1.0) - \sigma^I(1.0).\tag{25}$$

- Condition 2:

By subtracting the zeroth moment of smooth component from the zeroth moment of ENDF, we obtain the zeroth moment of singular component:

$$\sigma_0^{II} = \sigma_0 - \sigma_0^I.\tag{26}$$

If we use  $(1, \sigma^{II}(1.0))$  from Condition 1 and the zeroth moment of singular component  $\sigma_0^{II}$  from Condition 2 with Eqs.(23) and (24) respectively, then we get

$$\sigma^{II}(1.0) = K^{II} \tau^{II} \exp\{-\tau^{II}(1-1)\},\tag{27}$$

and

$$\sigma_0^{II} = 2\pi K^{II} h_0(\tau^{II}), \quad (28)$$

where

$$h_0(\tau^{II}) = 1 - \exp(-2\tau^{II}). \quad (29)$$

From Eq.(27), we obtain  $K^{II}$ :

$$K^{II} = \frac{\sigma^{II}(1.0)}{\tau^{II}}. \quad (30)$$

In order to determine  $\tau^{II}$ , we insert Eqs.(29) and (30) into Eq.(28), then we get nonlinear equation for  $\tau^{II}$ :

$$\tau^{II} \sigma_0^{II} - 2\pi \sigma^{II}(1.0) \{1 - \exp(-2\tau^{II})\} = 0. \quad (31)$$

$\tau^{II}$  can be obtained effectively by using Newton's method for solving Eq.(31). After obtaining the value of  $\tau^{II}$ , it is obvious that we can easily get  $K^{II}$  by using Eq.(30).

The restricted momentum transfer is calculated from the moments of the singular component as well:

$$\alpha = \sigma_0^{II} - \sigma_1^{II}. \quad (32)$$

An overview of the new method is displayed in Fig. 2.

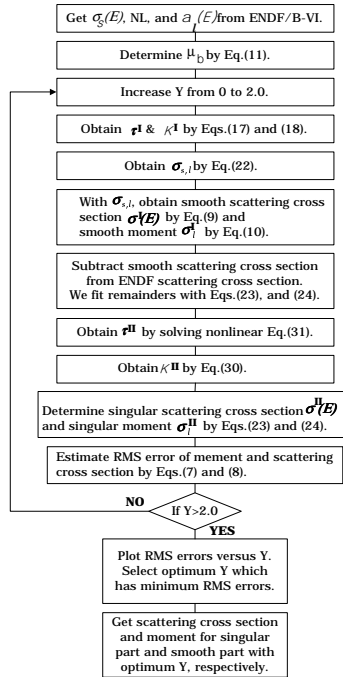


Figure 2: The procedure of the new method.

## 4. Numerical Tests and Results

### 4.1 Minimization of RMS errors

In Section 3.1, we introduced extrapolation exponential function. In order to determine parameters  $K^I$  and  $\tau^I$  for this function, we suggest an extra degree of freedom ( $Y$ ) which is determined by RMS errors: Eqs.(7) and (8). Doing numerical tests on several isotopes and energy, graphs of RMS errors of moment and scattering cross section versus  $Y$ , that is varying from 0 to 2.0, have three types of shape.

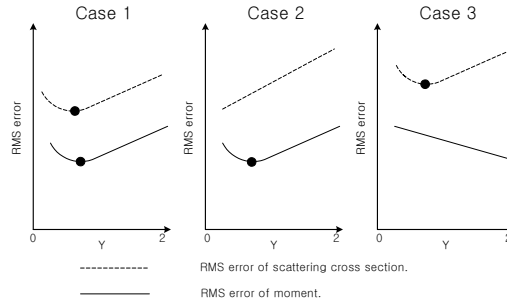


Figure 3: Three types of RMS error of scattering cross section and moment vs  $Y$ .

Dotted line and solid line in Fig. 3 represent RMS errors of scattering cross section and moment, respectively. This graph of RMS errors can be obtained by using Eqs.(7) and (8) with varying  $Y$  from 0 to 2.0.

In each case, we define  $Y$  in the following way.

- Case 1:  
We define  $Y$  as the average of two  $Y$ 's which have minimum RMS errors.
- Case 2:  
We define  $Y$  as the value which minimizes RMS error of moment.
- Case 3:  
We define  $Y$  as the value which minimizes RMS error of scattering cross section.

Tested isotopes and energy are shown in Table 1.

Table 1: Tested Isotopes and Energy

	Pb-206	U-235	U-238	Pu-239	Pu-240
14MeV			Case 1	Case 1	
15MeV		Case 1			Case 1
16MeV	Case 3		Case 1	Case 1	
17.5MeV					Case 1
20MeV	Case 3	Case 1	Case 2	Case 1	Case 1

As we can see, in the most tests, Case 1 is dominant. However, there are a few cases which are dominated by Case 2 or Case 3. In the next section, we represent computational results for each case.

## 4.2 Computational results

In this section, we present three results of the new decomposition method. We select three of them from Table 1. The first one is U-238 at energy  $14MeV$  for Case 1, the second one is U-238 at energy  $20MeV$  for Case 2, and the third one is Pb-206 at energy  $20MeV$  for Case 3. The reason for selecting U-238 at energy  $14MeV$  for Case 1 is that we want to compare C-L method with new method.

In these numerical tests, we use  $P_9$  approximation since all smooth moments are set to zero for  $l \geq 10$  in figures for moments. The  $\mu_b$  of each case is 0.65, 0.64 and 0.5976 respectively.

We attach ENDF data, which are used for the following three cases, in Table 5.

### 4.2.1 U-238 for Case 1

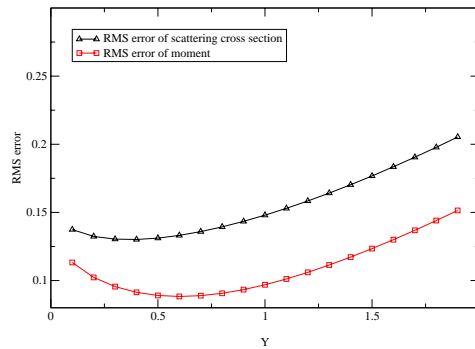


Figure 4: RMS error vs  $Y$ .

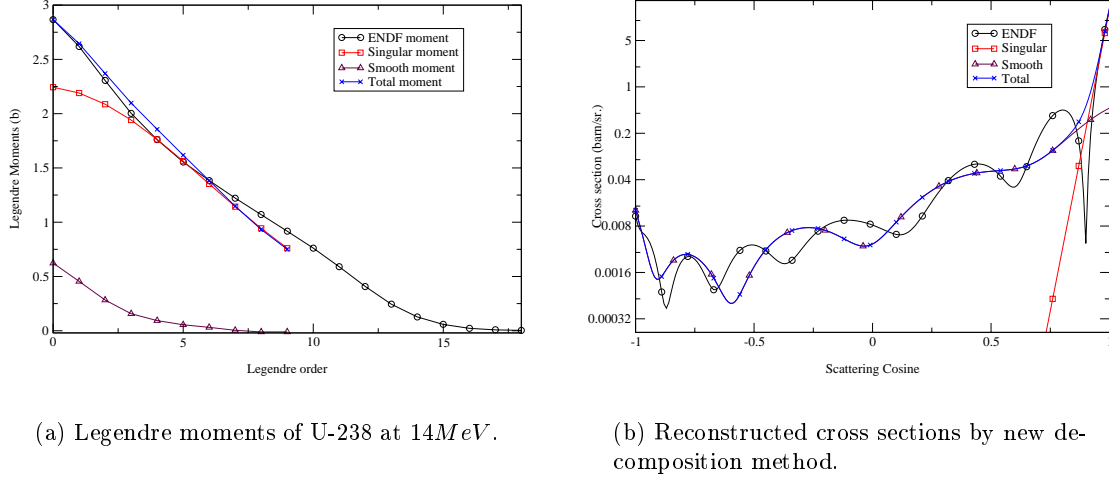
In Fig. 4, we get two  $Y$ 's. One is  $Y = 0.4$  which minimizes RMS error of scattering cross section, the other is  $Y = 0.6$  which minimizes RMS error of moment. We set  $Y$  as average of two  $Y$ 's for this case.

With  $Y = 0.5$ , we can determine the following variables in Table 2:

Table 2: The Parameters for Case 1

$\tau^I$	5.9330	$K^I$	0.0843	RMS error of moment	0.0890
$\tau^{II}$	41.9164	$K^{II}$	0.3571	RMS error of scattering cross section	0.1311

With the above parameters, we have calculated the moments of both singular and smooth cross section by using Eqs.(9), (10), (23), and (24). The results are displayed in Fig. 5.(a). We also display ENDF moment in the same domain to see the conservation of moments.



(a) Legendre moments of U-238 at 14MeV.

(b) Reconstructed cross sections by new decomposition method.

Figure 5: Reconstructed moments and cross sections by new decomposition method.

The sum  $\sigma_l = \sigma_l^I + \sigma_l^{II}$  matches well the ENDF moment. This means that our new approach is quite acceptable. For the restricted momentum transfer, we use the zeroth and the first moment of singular component. The momentum transfer  $\alpha$  is so important in the BFP equation that we need to pay attention to get the correct zeroth and first moment of singular component. In our new approach, we are always able to get correct momentum transfer since the zeroth moment of singular component is obtained by Eq.(26), even though we get singular and smooth moment independently.

In Fig. 5.(b), we see that decomposed singular and smooth scattering cross section by using our new approach. One sees that the main peak and smooth scattering cross section are well fitted. The ENDF elastic scattering, which is in Fig. 5.(b), uses  $P_{18}$  truncation to accurately model the whole elastic scattering cross section. However, we use only  $P_9$  truncation with almost the same accuracy.

This new approach looks similar to C-L method in that we use exponential function for singular component. However, a major difference is that we use Legendre expansion for smooth component to get more accurate representation of scattering cross section.

In Fig. 6, we see that the differences between the two methods, which are C-L method and our method. The data in ENDF, C-L method, and our new method are displayed in the same domain. Both methods fit forward peak well. However, when it comes to smooth scattering cross section, our new method gives better representation. If we consider ENDF as reference, the RMS error of both methods give more obvious results.

$$\text{RMS error} = \sqrt{\frac{1}{N} \sum_{i=1}^N \{P_i - \hat{P}_i\}^2}, \quad (33)$$

where  $P_i$  is scattering cross section,  $\hat{P}_i$  is reference, and  $N$  is number of check points. We used 200 check points.

The RMS errors are 0.1645 with C-L method and 0.1311 with our new method. If we

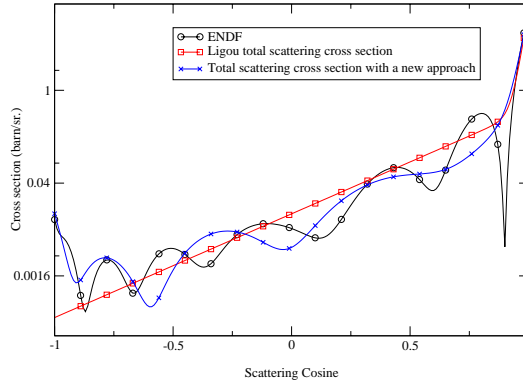


Figure 6: Total scattering cross section of C-L method and new method.

consider this result, we can say that this new approach is more advanced scattering decomposition method. In this section, we give more detail explanation since we want to compare with Caro and Ligou's test result. In the next two sections, we present only our test results.

#### 4.2.2 U-238 for Case 2

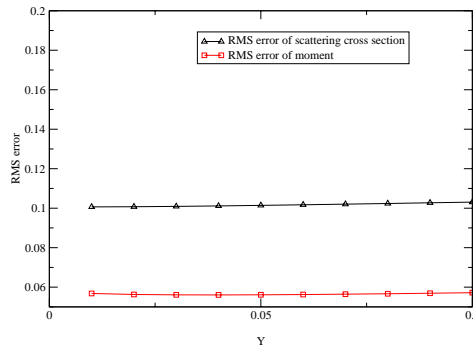


Figure 7: RMS error vs  $Y$ .

In Fig. 7, we get only one  $Y$  which minimizes RMS error of moment. From the graph of RMS error of scattering, we cannot get  $Y$  which minimizes RMS error of scattering. As we define  $Y$  in Section 4.1, we use 0.04 as the  $Y$  value.

With  $Y = 0.04$ , we can determine the following variables in Table 3:

Table 3: The Parameters for Case 2

$\tau^I$	3.1875	$K^I$	0.0125	RMS error of moment	0.0561
$\tau^{II}$	45.7146	$K^{II}$	0.5263	RMS error of scattering cross section	0.1012

The decomposed moment and scattering cross section of U-238 at  $20MeV$  are displayed in Figs. 8.(a) and 8.(b). The ENDF elastic scattering uses  $P_{20}$  truncation to accurately model the whole elastic scattering cross section. However, we use only  $P_9$  truncation with almost the same accuracy.

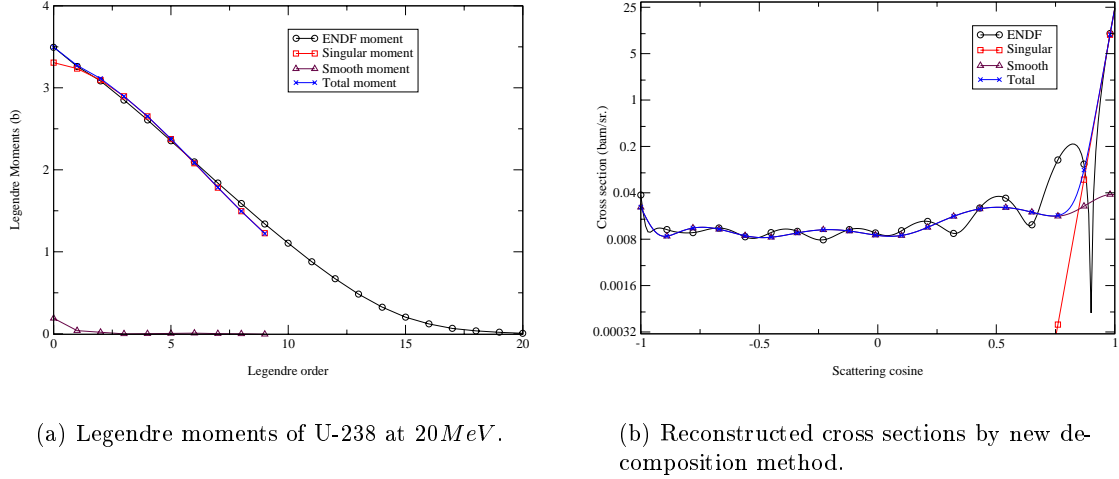


Figure 8: Reconstructed moments and cross sections by new decomposition method.

### 4.2.3 Pb-206 for Case 3

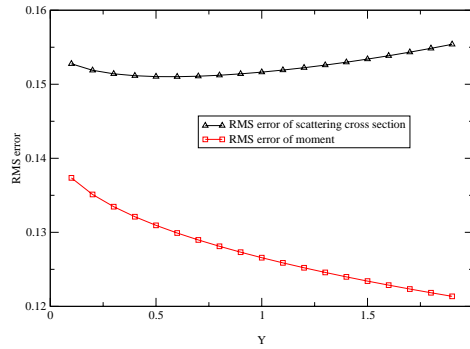


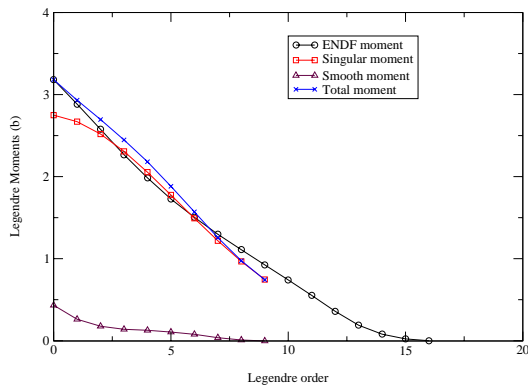
Figure 9: RMS error vs  $Y$ .

In Fig. 9, we get only one  $Y$  which minimizes RMS error of scattering. As we define  $Y$  in Section 4.1, we use 0.6 as the  $Y$  value.

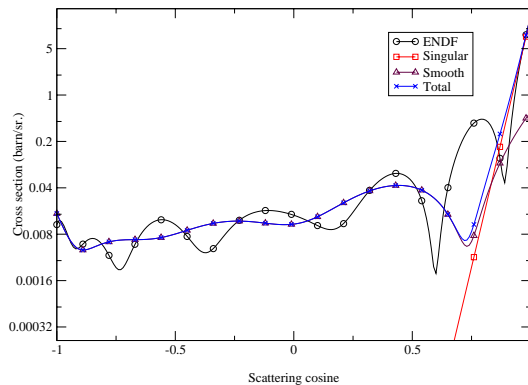
With  $Y = 0.6$ , we can determine the variables in Table 4. The decomposed moment and scattering cross section of Pb-206 at  $20MeV$  are displayed in Figs. 10.(a) and 10.(b).  $P_{15}$  truncation is used for ENDF to accurately model the whole elastic scattering cross section. However, we use only  $P_9$  truncation with almost the same accuracy.

Table 4: The Parameters for Case 3

$\tau^I$	14.1853	$K^I$	0.0423	RMS error of moment	0.1299
$\tau^{II}$	34.7759	$K^{II}$	0.4375	RMS error of scattering cross section	0.1510



(a) Legendre moments of Pb-206 at 20 MeV.



(b) Reconstructed cross sections by new decomposition method.

Figure 10: Reconstructed moments and cross sections by new decomposition method.

## 5. Conclusions

We have presented a new Fokker-Planck decomposition technique for highly anisotropic scattering cross section. The C-L method and the MB method construct the moments of the smooth component directly from the moments of the complete cross section which is a truncated Legendre expansion. In order to get more accurate BFP data, it is necessary to start from the basic data  $\sigma_s(\mu)$  (given by ENDF/B-VI which is the latest version) like the PRF method. However, the PRF method is somewhat inadequate to deal with the neutron scattering cross section since its shape is irregular. In our new approach, we make the most of characteristics of exponential function and Legendre expansion. The exponential function is used for representing forward-peaked scattering cross section, and Legendre expansion is used for representing smooth scattering cross section.

The extrapolation exponential function in smooth component plays an important role to couple the exponential function and the Legendre expansion. That is to say, an extra degree of freedom  $Y$ , which is introduced in the extrapolation exponential function, is closely related to conserve scattering moment and scattering cross section as well.

Overall, we conclude that our new approach for decomposition is a good alternative to the previous decomposition methods. It is superior to the other methods in terms of accuracy and applicability.

Table 5: ENDF Data for Each Case

	CASE 1	CASE 2	CASE 3
Isotope	U-238	U-238	Pb-206
Energy	14MeV	20MeV	20MeV
NL	18	20	15
$\sigma_s(E)$	2.867296	3.496053	3.1818
$a_0$	1.0	1.0	1.0
$a_1$	9.133300e-01	9.328200e-01	9.063900e-01
$a_2$	8.040000e-01	8.819240e-01	8.095800e-01
$a_3$	6.987100e-01	8.156340e-01	7.126500e-01
$a_4$	6.136700e-01	7.462500e-01	6.238000e-01
$a_5$	5.422700e-01	6.730930e-01	5.427000e-01
$a_6$	4.828500e-01	6.000610e-01	4.729000e-01
$a_7$	4.262700e-01	5.259340e-01	4.077900e-01
$a_8$	3.729400e-01	4.543000e-01	3.486600e-01
$a_9$	3.198400e-01	3.833050e-01	2.905300e-01
$a_{10}$	2.655200e-01	3.161720e-01	2.328400e-01
$a_{11}$	2.054300e-01	2.514430e-01	1.738100e-01
$a_{12}$	1.422400e-01	1.920600e-01	1.128300e-01
$a_{13}$	8.548100e-02	1.381670e-01	5.939900e-02
$a_{14}$	4.437900e-02	9.321990e-02	2.517700e-02
$a_{15}$	2.025800e-02	5.794970e-02	7.025800e-03
$a_{16}$	7.760600e-03	3.430310e-02	
$a_{17}$	2.818900e-03	1.864920e-02	
$a_{18}$	1.108600e-03	1.030530e-02	
$a_{19}$		5.086290e-03	
$a_{20}$		1.725920e-03	

### Acknowledgement

This work was supported in part by the Ministry of Science and Technology of Korea through the National Research Laboratory (NRL) Program.

### References

- [1] M. Caro and J. Ligou, "Treatment of Scattering Anisotropy of Neutrons Through the Boltzmann-Fokker-Planck Equation," *Nucl. Sci. Eng.*, **83**, 242 (1983).
- [2] J.E. Morel, "Angular Fokker-Planck Decomposition and Representation Techniques," *Nucl. Sci. Eng.*, **103**, 1 (1989).

- [3] R.E. MacFarlane and D.W. Muir, "The NJOY Nuclear Data Processing System, Version 91," *Los Alamos National Laboratory* (Dec. 1994).
- [4] V. McLane, C.L. Dunford, and P.F. Rose, "ENDF-102 Data Formats and Procedures for the Evaluated Nuclear Data File ENDF-6," *BNL-NCS-44945, Rev.2/97, Brookhaven National Laboratory* (Jul. 1990).
- [5] N.Z. Cho and S.G. Hong, *Neutron Transport Theory - Computational Algorithms and Applications*, Chungmoongak (2000) (in Korean).
- [6] Nam Zin Cho, "Boltzmann-Fokker-Planck Equation for Charged Particle Transport," in *Neutron and Radiation Transport Simulation: Theory and Applications*, edited by N.Z. Cho, Korea Advanced Institute of Science and Technology (2001).